ACS APPLIED MATERIALS & INTERFACES

www.acsami.org

Research Article

Enhanced Sensing Performance of a Microchannel-Based Electrochemiluminescence Biosensor for Adenosine Triphosphate via a dsDNA Superstructure Amplification Strategy

Yanling Huang, Weixin Li, Jianping Zheng,* Fang Luo, Bin Qiu, Jian Wang, Cuiying Lin,* and Zhenyu Lin*

Cite This: *ACS Appl. Mater. Interfaces* 2022, 14, 37222−37228

Read Online

ACCESS | Metrics & More | Article Recommendations

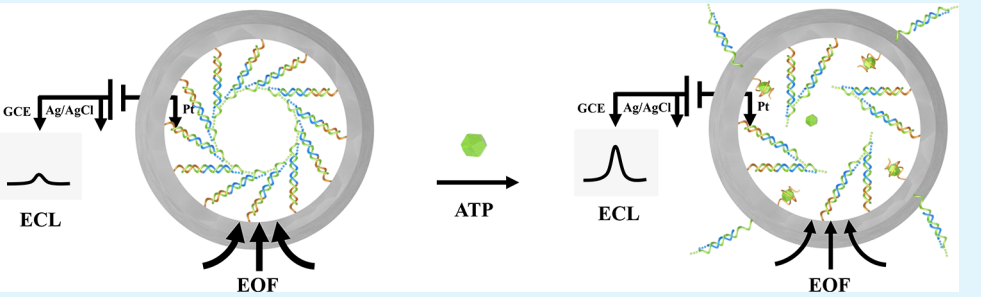

ABSTRACT: The sensing performance of a microchannel-based electrochemiluminescence (ECL) biosensor is related to the change ratio of charge density on the surface of microchannels caused by a target recognition reaction. In this study, adenosine triphosphate (ATP) served as a model target. The dsDNA superstructures containing a capture probe (CP, containing an ATP aptamer sequence) and alternating units of ssDNA probes of P1 and P2, CP/$(P1/P2)_n$, were grafted onto the inner wall of microchannels first. The CP in dsDNA superstructures captured ATP molecules, causing the release of dsDNA fragments containing alternating units of P1 and P2, $(P1/P2)_n$. The target recognition reaction significantly changed the charge density of microchannels, which altered the ECL intensity of the (1,10-phenanthroline)ruthenium(II)/tripropylamine system in the reporting interface. The ECL intensity of the constructed system had a linear relationship with the logarithm of ATP concentration ranging from 1 fM to 100 pM with a detection limit of 0.32 fM (S/N = 3). The biosensor was successfully applied to detect ATP in rat brains.

KEYWORDS: *charge density, microchannel, amplification, electrochemiluminescence, adenosine triphosphate*

1. INTRODUCTION

An artificial microchannel has been coupled with electrochemiluminescence (ECL) technology to construct a microchannel-based ECL sensing platform.[1,2] Different from the traditional ECL detection system,[3−5] the ECL intensity of the luminophore/coreactant system can be altered by the charge density in microchannels. The change ratio of charge density has a great effect on its sensing performance; the greater the change in the charge density of microchannels in the presence of the target, the higher the sensitivity of the system. But in the previously reported two systems, the change ratio of charge density caused by a target recognition reaction was limited. There is an urgent need to find some approaches to improve the performance of the system.

Many amplification strategies have been designed to enhance the sensing performance of channel-based electrical sensing.[6−8] For example, Jiang and co-workers integrated a concatemer with a larger number of charges and multiple aptamer sequences on the inner wall of a nanochannel; the target bound to the aptamer sequence and melted the DNA concatemers, and the fully stuffed and opened nanochannel exhibited an extremely high gating ratio.[9−11] Liu and co-workers provided a built-in amplification mechanism via a target DNA-triggered hybridization event to create long concatemers on the inner surface of the nanochannel; this strategy can cause a significant change in charge density after the addition of targets and result in the enhancement of the detection sensitivity of the system.[11,12] Increasing the change ratio can improve the sensing performance; if this character can be applied in the microchannel-based ECL biosensing

Received: June 17, 2022
Accepted: July 25, 2022
Published: August 2, 2022

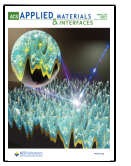

https://doi.org/10.1021/acsami.2c10776
ACS Appl. Mater. Interfaces 2022, 14, 37222−37228

Scheme 1. (a) Schematic Illustration of the Microchannel-Based ECL Biosensor Setup. (b) Preparation of CP/$(P1/P2)_n$ Superstructures. (c) Principle of the Biosensor for ATP Detection via a dsDNA Superstructure Amplification Strategy.

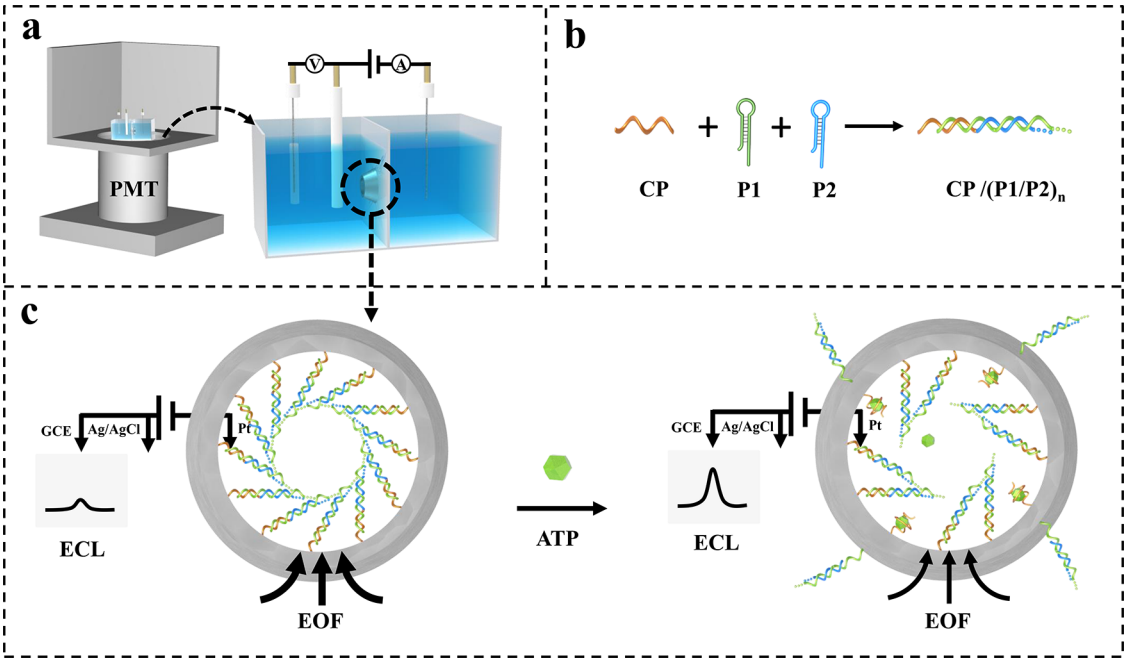

platform, the biosensing performance of the system can be enhanced greatly.

Adenosine triphosphate (ATP), one of the chemical indicators in energy metabolism and signal transduction, is considered as a disease marker. Therefore, it is of great significance to identify and detect ATP.[13−15] In this study, the dsDNA superstructures containing a capture probe (CP, containing an ATP aptamer sequence) and alternating units of ssDNA probes of P1 and P2, CP/$(P1/P2)_n$, were prepared and grafted onto the inner wall of the microchannel. In the presence of ATP, the CP in CP/$(P1/P2)_n$ captured ATP, causing $(P1/P2)_n$ fragments to be released from the surface. The target recognition reaction caused a significant change in charge density and ECL emission, which enhanced the performance of the microchannel-based ECL system. The proposed biosensor has been successfully applied to detect ATP in rat brains.

2. EXPERIMENTAL SECTION

2.1. Chemicals and Reagents. The borosilicate capillaries (B150-86-10) were obtained from Sutter Instrument. Capture probe (CP): 5′-NH_2-$(CH_2)_6$-TTT TTT TTT ACC TGG GGG AGT ATT GCG GAG GAA GGT-3′, probe DNA1 (P1): 5′-GTG TTA TTG CGG AGG TAC CTT CCT CCG CAA TAG TG-3′, probe DNA2 (P2): 5′-ACC TCC GCA ATA ACA CCA CTA TTG CGG AGG AAG GT-3′, phosphate-buffered saline (PBS) buffer, and streptavidin-modified magnetic beads (MBs) were obtained from Sangon Biotech (Shanghai, China). Dimethyl sulfoxide (DMSO), tris(hydroxymethyl) aminomethane (Tris), inorganic salts (i.e., KCl, NaCl, $(NH_4)_2S_2O_8$, $MgCl_2$, and $CaCl_2$), and ethanol (C_2H_5OH) were purchased from Sinopharm Chemical Reagent (Shanghai, China). Uridine triphosphate (UTP), ATP, 1-ethyl-3-(3′-dimethylaminopropyl) carbodiimide (EDC), cytosine triphosphate (CTP), (1,10-phenanthroline)-ruthenium(II) [$Ru(phen)_3^{2+}$], guanosine triphosphate (GTP), 3-aminopropyltriethoxysilane (APTES), adenosine monophosphate (AMP), succinic anhydride (SA), adenosine 5′-diphosphate (ADP), *N*-hydroxysuccinimide (NHS), and tripropylamine (TPrA) were provided by Sigma-Aldrich (Shanghai, China).

2.2. Fabrication and Functionalization of Microchannels. The borosilicate capillaries were pretreated with piranha solution first. Then, the pretreated borosilicate capillaries were heated and pulled with a micropipette puller (P-2000g, made by Sutter Instrument) to obtain conical microchannels; the diameter and the cone half angle of the conical microchannel were 3 μm and 5°, respectively. After this, the bare conical microchannels were backfilled with APTES (10%, in ethanol) and SA (0.01 g mL^{-1}, in DMSO) solution, respectively, to prepare carboxyl group-functionalized microchannels.[1,16] The CP (1 μM), P1 (1 μM), and P2 (1 μM) were mixed at 37 °C for 3 h to form dsDNA superstructures. Then, carboxyl-modified microchannels were backfilled with PBS buffer (pH = 7.0) containing EDC (2 mg mL^{-1}), NHS (1 mg mL^{-1}), and dsDNA superstructures for 10 h. The dsDNA superstructure-functionalized microchannels were obtained after washing.

2.3. Electrochemical and ECL Measurements. The ion transport behavior in microchannels was measured using two Ag/AgCl electrodes in KCl solution (10 mM). The current−voltage (*I*−*V*) curves were measured by cyclic voltammetry scanning; the potential ranged from −1.0 to 1.0 V, and the scan rate was 50 mV s^{-1}.

The detection system is the same as previously reported.[1] For target detection, the recognition elements on the surface of microchannels reacted with ATP solution with different concentrations first. Then, ECL spectra (voltage of photomultiplier tube, −650 V) were recorded using a three-electrode system in bulk solution (0.5 M KCl, 10 mM Tris, 5 μM $Ru(phen)_3^{2+}$, and 13 mM TPrA). The scanning voltage ranged from 0.4 to 1.6 V. The parallel experiments were conducted at least three times.

2.4. In Vivo Microdialysis. In vivo microdialysis experiments were performed according to previous work.[13,17] Adult male Sprague−Dawley rats (250−300 g) were obtained from the Experimental Animal Center of Fuzhou University (Fuzhou, China). The rats were anesthetized and then placed in a stereotaxic framework. The body temperature of the rats was maintained at 37 °C. A guide cannula was implanted into the rat cerebral cortex, and then the position was fixed with dental cement and three small screws. A microdialysis probe was implanted into the guide cannula to perfuse artificial cerebrospinal fluid solution at 1.0 μL min^{-1} to collect the microdialysate. The microdialysate was stored at −20 °C before use. Animal surgery protocols were approved by the Ethics Committee of

https://doi.org/10.1021/acsami.2c10776
ACS Appl. Mater. Interfaces 2022, 14, 37222−37228

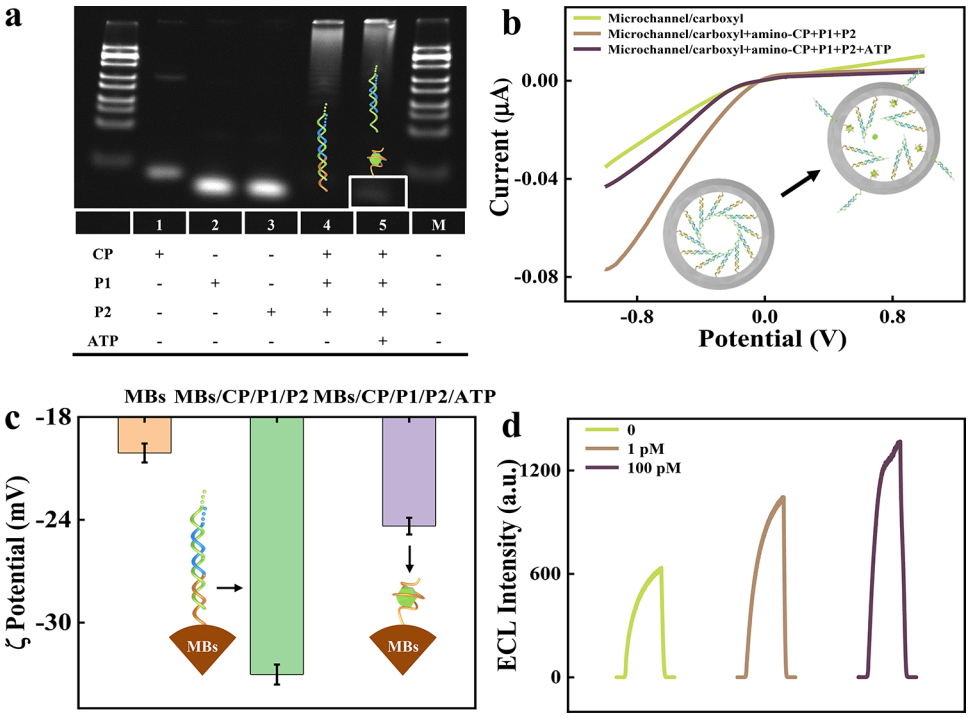

Figure 1. (a) Gel electrophoresis images. Lanes 1−4: CP (#1), P1 (#2), P2 (#3), CP + P1 + P2 (#4), and CP + P1 + P2 + ATP (#5). (b) Characterization of ionic transport in the carboxyl-functionalized microchannel, dsDNA superstructure-functionalized microchannel, and dsDNA superstructures + ATP-functionalized microchannel. (c) ζ potentials of functionalized MBs before and after the addition of ATP. (d) Feasibility of the proposed biosensor, and the concentrations of ATP solution were 0, 1, and 100 pM.

Experimental Animals of Fuzhou University (approval no. 2020-SG-001).

3. RESULTS AND DISCUSSION

3.1. Principle of the Proposed System Based on a dsDNA Superstructure Amplification Strategy. The experimental device included a dsDNA superstructure-functionalized microchannel and a three-electrode system (Ag/AgCl, GCE, and Pt). The functionalized microchannel was used as a target recognition reaction site, and GCE served as an ECL reporting interface. The Pt electrode was placed in the base end of the microchannel, and the GCE and Ag/AgCl electrode were placed on the tip side of the microchannel. The functionalized microchannel with high resistance resulted in a correlation between ionic current and the interfacial properties of the microchannel, and charge balance permits the correlation between ionic current and ECL emission.[1,18] Therefore, the ECL intensity of the $Ru(phen)_3^{2+}$/TPrA system was altered by the interfacial properties of the microchannel (Scheme 1a). To assemble dsDNA superstructures in the inner wall of the microchannel, dsDNA superstructures were first prepared outside the microchannel. Amino-labeled CP can hybridize with P1 with a toehold-mediated strand displacement reaction to expose the ssDNA region within P1, which can further hybridize to P2 via secondary toehold-mediated DNA strand displacement to expose a new ssDNA region within P2. The ssDNA region within P2 can also hybridize to P1 to trigger the next circulation until P1 or P2 is exhausted. The product of the DNA hybridization reaction was a long concatemer, named $CP/(P1/P2)_n$ (Scheme 1b).

Amino-labeled $CP/(P1/P2)_n$ was grafted onto the inner wall of the carboxyl-functionalized surface through an EDC/NHS coupling reaction. The modification of $CP/(P1/P2)_n$ on the inner surface of the microchannel significantly increased the negative charge density because DNA is rich in phosphate skeleton. The negatively charged surface generated electroosmotic flow (EOF) toward the cathode driven by the external electrical field, and the EOF induced the transport of ions from the tip to the base, which depleted the ionic concentration at the tip; the phenomenon has been confirmed in our previous work.[1] In the absence of ATP, the generation of EOF in the $CP/(P1/P2)_n$-functionalized microchannel with high negative charge density depleted the ionic concentration at the tip of the microchannel, and a weak ECL emission was detected. The CP in $CP/(P1/P2)_n$ can capture ATP molecules because CP contains the aptamer sequence for ATP molecules. ATP will replace $(P1/P2)_n$ on the inner wall of the microchannel, and the negative charge density will decrease greatly. This change caused a decrease in the EOF, thereby accumulating ionic concentration at the tip, and an increase in ECL emission can be obtained. (Scheme 1c). The dsDNA superstructure-functionalized microchannel significantly changed the negatively charged density on the inner wall of the microchannel to improve the detection sensitivity.

3.2. Feasibility Test of the Microchannel-Based ECL Biosensor for ATP Detection. The formation of dsDNA superstructures and their melting by ATP molecules was confirmed by 12% gel electrophoresis (Figure 1a). Lanes 1−5 represent CP (#1), P1 (#2), P2 (#3), CP + P1 + P2 (#4), and CP + P1 + P2 + ATP (#5), respectively. Compared with lanes 1−3, a bright band was observed at the tip of lane 4; the analysis indicated that CP, P1, and P2 can form the high-molecular-weight dsDNA superstructures, $CP/(P1/P2)_n$. After being treated with ATP molecules, a CP band was observed at the bottom of lane 5 because CP contained an ATP aptamer sequence and ATP can bind with CP in dsDNA super-

https://doi.org/10.1021/acsami.2c10776
ACS Appl. Mater. Interfaces 2022, 14, 37222−37228

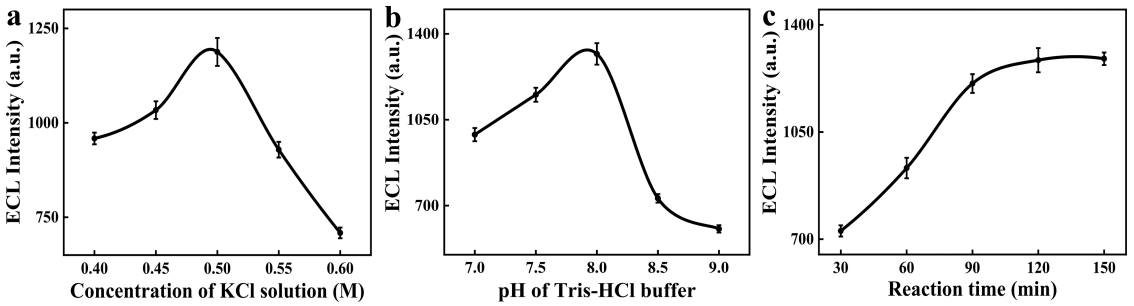

Figure 2. Effect of (a) ionic strength, (b) pH of Tris−HCl buffer, and (c) the reaction time of the target recognition reaction between dsDNA superstructures and ATP molecules on ECL emission. The concentration of ATP solution was 100 pM.

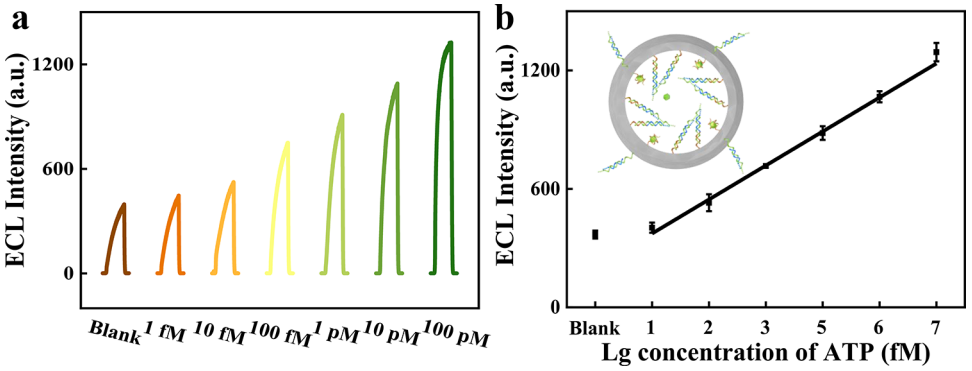

Figure 3. (a) ECL spectra of ATP at different concentrations. (b) Relationship between ECL emission and the logarithmic concentration of ATP (lg C_{ATP}) was obtained. The ECL spectra were obtained by immersing dsDNA superstructure-functionalized microchannels into ATP solution with different concentrations: 0 fM, 1 fM, 10 fM, 100 fM, 1 pM, 10 pM, and 100 pM.

structures to form the CP/ATP complex, which can cause the release of $(P1/P2)_n$ from CP/$(P1/P2)_n$. The results demonstrated that ATP can bind to CP in CP/$(P1/P2)_n$ to achieve a target recognition reaction.

The *I*−*V* curves were measured to characterize the assembly of different elements in the microchannel (Figure 1b). The *I*−*V* curves of the functionalized microchannels show obvious ionic current rectification, and the ionic current recorded at a negative potential was higher than that at a positive potential. Compared with the ionic current in the carboxyl-functionalized microchannel, the ionic current at the negative potential increased and the ionic current at the positive potential decreased in the dsDNA superstructure-functionalized microchannel. The reasons are as follows: at the negative potential, the negative charge density surface promoted cation accumulation at the tip of the microchannel, and the microchannel was in a high conductance state. However, at the positive potential, the charged surface caused cation depletion at the tip of the microchannel, and the microchannel was in a low conductance state. The change in ionic current demonstrated the successful assembly of the dsDNA superstructure on the inner surface of the microchannel. The phenomena have been confirmed in previous work.[19,20] Then, the ionic current at the negative potential decreased after treating the dsDNA superstructure-functionalized microchannel with ATP. Because dsDNA superstructures contained the ATP aptamer sequence (CP), and ATP molecule may trigger the release of $(P1/P2)_n$ from the inner wall of the microchannel. The ATP recognition reaction resulted in a significant decrease in the negative charge density of the microchannel. The results demonstrated the successful assembly of different elements in the microchannel.

To further confirm the regulation of the negative charge density of the dsDNA superstructure-functionalized interface by ATP, ζ potential measurements were performed. The ζ potential of streptavidin-modified magnetic beads (MBs) was negative because streptavidin can dissociate a larger number of $-COO^-$ in the neutral condition. The ζ potential value of dsDNA superstructure-functionalized MBs was higher than that of streptavidin-functionalized MBs. The results demonstrated that biotin-modified CP was grafted onto the surface of streptavidin-functionalized MBs, and then the alternating units of P1 and P2 grew from the CP on the streptavidin-modified MBs surface to create dsDNA superstructures, which efficiently increased the ζ potential of the functionalized MBs. In the presence of ATP, the ζ potential value decreased (Figure 1c). The results further demonstrated that the charge density of dsDNA superstructure-functionalized MBs can be regulated by an ATP recognition reaction.

The dsDNA superstructure-functionalized microchannels reacted with ATP with different concentrations (1 pM and 1 nM) to assess the feasibility of the proposed system. Figure 1d shows the ECL intensity of the dsDNA superstructure-functionalized microchannel after immersing in ATP solution with different concentrations. The combination of ATP molecules with CP in CP/$(P1/P2)_n$ caused $(P1/P2)_n$ fragments to be released from the inner wall of the microchannel, which significantly decreased the negative charge density. The negatively charged surface generated EOF toward the cathode driven by the external electrical field, and the strength of EOF decreased after the target recognition reaction, causing the accumulation of ions at the tip, and thus the ECL emission increased. Hence, the ECL emission responded to ATP concentration. These results validated

https://doi.org/10.1021/acsami.2c10776
ACS Appl. Mater. Interfaces 2022, 14, 37222−37228

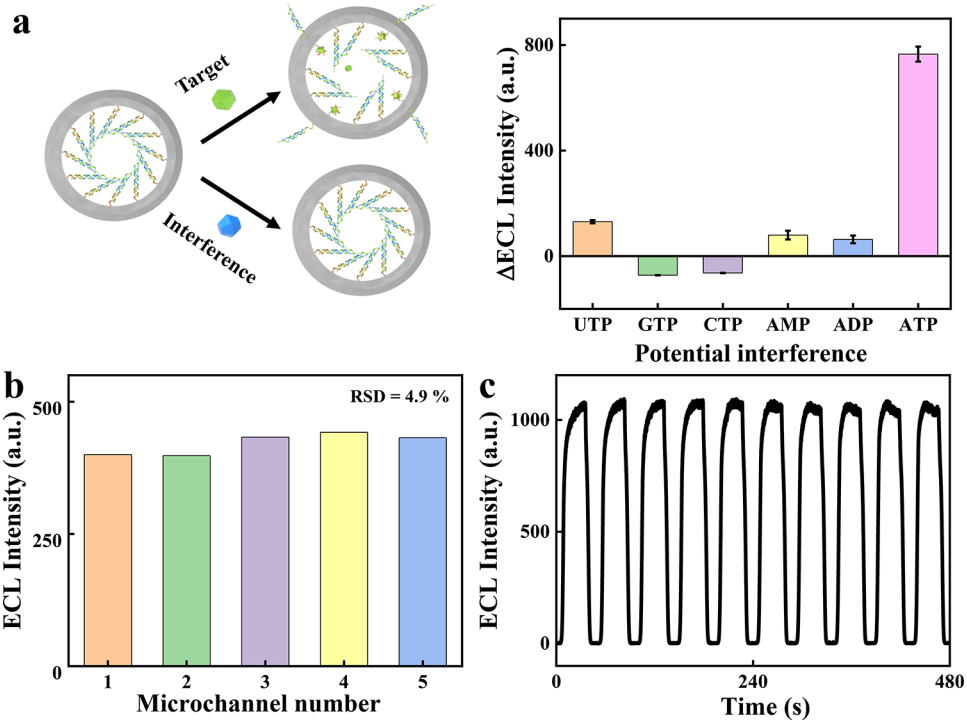

Figure 4. (a) Selectivity measurement of the constructed method. The concentration of ATP and interference substances was 10 pM and 10 nM, respectively. (b) Reproducibility measurement of five dsDNA superstructure-functionalized microchannels. (c) Stability measurement of the constructed method; the concentration of ATP was 10 pM.

that the dsDNA superstructure-modified microchannel can be used for the ATP recognition reaction.

3.3. Optimization of Experimental Conditions of the Microchannel-Based ECL Biosensor for ATP Detection. The experimental conditions were optimized to enhance the sensing performance of the microchannel-based ECL biosensor for ATP detection, such as ionic strength, pH of Tris−HCl buffer, and the reaction time between dsDNA superstructures and ATP molecules. The ionic concentration of KCl solution and pH of Tris−HCl buffer not only affect the luminescence efficiency of the $Ru(phen)_3^{2+}$/TPrA system but also affect the EOF strength in the charged microchannel. The ionic current increased, and the EOF decreased with the increase of the KCl concentration. Therefore, the effect of KCl concentration on ECL intensity was studied first. Figure 2a shows the relationship between the ECL intensity and KCl concentration in bulk solution from 0.4 to 0.6 M. It clearly shows that the ECL intensity reached the maximum value when the concentration of KCl was 0.5 M. Then, the influence of pH on ECL intensity was studied. The signal increased with the increase of pH and then decreased when the pH was more than 8.0 (Figure 2b). Figure 2c shows the effect of ATP recognition reaction time on ECL intensity; the signal reached a plateau after 90 min. So, the optimized KCl concentration was 0.5 M, the optimized pH was 8.0, and the optimized time of target recognition reaction was 90 min; those experiment conditions were used in subsequent experiments.

3.4. Analysis Performance of the Microchannel-Based ECL Biosensor. The analysis performance of the constructed method was evaluated under the optimized experimental conditions. ECL emission of the proposed systems increased with the increase of ATP concentration (Figure 3a). The proposed method has a linear relationship between ECL intensity (I_{ECL}) and lg C_{ATP} in the range of 1 fM to 100 pM (Figure 3b), and it can be represented as

$$I_{ECL} = 177.8 \lg C_{ATP} + 201.67, \quad R^2 = 0.992$$

The limit of detection (LOD) was 0.32 fM (S/N = 3). R represents the correlation coefficient. The detection of ATP with high sensitivity can be attributed to the significant change in negative charge density after the addition of the target, which provided a signal amplification strategy for target detection.

3.5. Selectivity, Reproducibility, and Stability Test. The selectivity is an important index of microchannel-based ECL biosensors, and the selectivity of the proposed system for the ATP assay was determined. The microchannel-based ECL biosensor has a highly selective response toward ATP without interference from its analogues, such as UTP, GTP, CTP, AMP, and ADP. There was an obvious ECL intensity change after adding 10 pM ATP into the functionalized microchannel, while almost no ECL intensity change was recorded after adding 10 nM interference substances (Figure 4a). The results indicated that the biosensor can be applied to detect ATP with high selectivity.

Parallel experiments on dsDNA superstructure-functionalized microchannel were repeated at least five times, and the relative standard deviation (RSD) of the ECL intensity was 4.9%, which presented a favorable reproducibility for the ATP assay (Figure 4b). The stability of functionalized microchannel was assessed by continuous scanning for 10 cycles, and the ECL intensity of scanning for 10 cycles was stable (Figure 4c), demonstrating the satisfactory stability of the constructed sensor.

3.6. Application of the Proposed Biosensor for ATP Detection in Rat Brains. The cortex of rat brains was selected as the sample to study the potential application of the

https://doi.org/10.1021/acsami.2c10776
ACS Appl. Mater. Interfaces 2022, 14, 37222−37228

constructed biosensor for target detection. The samples were diluted 10^6 times for testing, and the results are presented in Table 1. The concentration of ATP in the cortex of rat brains ranged from 4.2 to 5.4 nM. The standard addition method was applied to test the accuracy of the proposed system, and two levels of ATP standard solution were added to the real samples. The recovery rates were in the range of 87.0 to 109.0%, and the RSD was below 8.0% (n = 5). The results demonstrated that the constructed system has potential application in the detection of ATP in rat brains.

Table 1. Detection of ATP in the Rat Brain by the Proposed Biosensor (n = 5)[a]

sample	added (pM)	found (pM)	recovery rate (%)	RSD (%)
1	0	0.0042	-	7.1
	0.6	0.60	99.3	1.3
	10.0	8.7	87.0	1.7
2	0	0.0054	-	4.4
	0.6	0.66	109.0	2.6
	10.0	8.8	87.9	2.8
3	0	0.0051	-	8.0
	0.6	0.59	97.5	1.2
	10.0	10.5	104.9	6.4

[a]"-" represents applicable.

4. CONCLUSIONS

In conclusion, dsDNA superstructures were applied to increase the change ratio of charge density of the microchannel to enhance the sensing performance of the microchannel-based ECL biosensor. The target recognition reaction can cause a significant change in the negative charge density and further significantly affect the ECL emission in the reporting interface, which improves the detection sensitivity. The constructed microchannel-based ECL biosensor can be applied to detect ATP in rat brains with satisfactory results. This amplification strategy not only achieves a highly sensitive detection of the target but also provides a new method for the screening of disease markers.

AUTHOR INFORMATION

Corresponding Authors

Jianping Zheng − *Department of Oncology, Shengli Clinical Medical College of Fujian Medical University, Fujian Provincial Hospital, Fuzhou 350001 Fujian, China*; Email: fjslzjp@sina.com

Cuiying Lin − *Ministry of Education Key Laboratory for Analytical Science of Food Safety and Biology, Fujian Provincial Key Laboratory of Analysis and Detection for Food Safety, College of Chemistry, Fuzhou University, Fuzhou 350116 Fujian, China*; Email: lcuiying@fzu.edu.cn

Zhenyu Lin − *Ministry of Education Key Laboratory for Analytical Science of Food Safety and Biology, Fujian Provincial Key Laboratory of Analysis and Detection for Food Safety, College of Chemistry, Fuzhou University, Fuzhou 350116 Fujian, China*; orcid.org/0000-0001-7890-6812; Email: zylin@fzu.edu.cn

Authors

Yanling Huang − *Ministry of Education Key Laboratory for Analytical Science of Food Safety and Biology, Fujian Provincial Key Laboratory of Analysis and Detection for Food Safety, College of Chemistry, Fuzhou University, Fuzhou 350116 Fujian, China*

Weixin Li − *Ministry of Education Key Laboratory for Analytical Science of Food Safety and Biology, Fujian Provincial Key Laboratory of Analysis and Detection for Food Safety, College of Chemistry, Fuzhou University, Fuzhou 350116 Fujian, China*

Fang Luo − *College of Biological Science and Engineering, Fuzhou University, Fuzhou 350116 Fujian, China*

Bin Qiu − *Ministry of Education Key Laboratory for Analytical Science of Food Safety and Biology, Fujian Provincial Key Laboratory of Analysis and Detection for Food Safety, College of Chemistry, Fuzhou University, Fuzhou 350116 Fujian, China*

Jian Wang − *Ministry of Education Key Laboratory for Analytical Science of Food Safety and Biology, Fujian Provincial Key Laboratory of Analysis and Detection for Food Safety, College of Chemistry, Fuzhou University, Fuzhou 350116 Fujian, China*

Complete contact information is available at: https://pubs.acs.org/10.1021/acsami.2c10776

Author Contributions

Y.H. and Z.L. conceived and designed the experiment; Y.H. and W.L. performed the experiments and collected the data; and Y.H., W.L., J.Z., F.L., J.W., B.Q., C.L., and Z.L. analyzed and discussed the data. All authors have given approval to the final version of the manuscript

Notes

The authors declare no competing financial interest.

ACKNOWLEDGMENTS

This project was supported by the National Natural Sciences Foundation of China (21974020).

REFERENCES

(1) Huang, Y.; Lu, Y.; Huang, X.; Wang, J.; Qiu, B.; Luo, F.; Lin, Z. Design of an Electrochemiluminescence Detection System Through the Regulation of Charge Density in a Microchannel. *Chem. Sci.* **2021**, *12*, 13151−13157.

(2) Huang, Y.; Luo, F.; Wang, J.; Wang, L.; Qiu, B.; Lin, C.; Lin, Z. Electrochemiluminescence Aptasensor for Charged Targets through the Direct Regulation of Charge Density in Microchannels. *Anal. Chem.* **2021**, *93*, 17127−17133.

(3) Li, S.; Zhang, D.; Liu, J.; Cheng, C.; Zhu, L.; Li, C.; Lu, Y.; Low, S.; Su, B.; Liu, Q. Electrochemiluminescence on Smartphone with Silica Nanopores Membrane Modified Electrodes for Nitroaromatic Explosives Detection. *Biosens. Bioelectron.* **2019**, *129*, 284−291.

(4) Lu, H.; Pan, J.; Wang, Y.; Ji, S.; Zhao, W.; Luo, X.; Xu, J.; Chen, H. Electrochemiluminescence Energy Resonance Transfer System between RuSi Nanoparticles and Hollow Au Nanocages for Nucleic Acid Detection. *Anal. Chem.* **2018**, *90*, 10434−10441.

(5) Liu, R.; Liu, C.; Li, H.; Liu, M.; Wang, D.; Zhang, C. Bipolar Electrochemiluminescence on Thread: A New Class of Electroanalytical Sensors. *Biosens. Bioelectron.* **2017**, *94*, 335−343.

(6) Zhang, J.; Zhang, L.; Li, Z.; Zhang, Q.; Li, Y.; Ying, Y.; Fu, Y. Nanoconfinement Effect for Signal Amplification in Electrochemical Analysis and Sensing. *Small* **2021**, *17*, No. 2101665.

(7) Ma, Q.; Li, Y.; Wang, R.; Xu, H.; Du, Q.; Gao, P.; Xia, F. Towards Explicit Regulating-ion-transport: Nanochannels with Only Function-elements at Outer-surface. *Nat. Commun.* **2021**, *12*, No. 1573.

(8) Ma, Q.; Liu, T.; Xu, R.; Du, Q.; Gao, P.; Xia, F. Revealing the Critical Role of Probe Grafting Density in Nanometric Confinement

in Ionic Signal via an Experimental and Theoretical Study. *Anal. Chem.* **2021**, *93*, 1984−1990.
(9) Jiang, Y.; Liu, N.; Guo, W.; Xia, F.; Jiang, L. Highly-Efficient Gating of Solid-State Nanochannels by DNA Supersandwich Structure Containing ATP Aptamers: A Nanofluidic IMPLICATION Logic Device. *J. Am. Chem. Soc.* **2012**, *134*, 15395−15401.
(10) Jiang, Y.; Feng, Y.; Su, J.; Nie, J.; Cao, L.; Mao, L.; Jiang, L.; Guo, W. On the Origin of Ionic Rectification in DNA-Stuffed Nanopores: The Breaking and Retrieving Symmetry. *J. Am. Chem. Soc.* **2017**, *139*, 18739−18746.
(11) Li, X.; Zhai, T.; Gao, P.; Cheng, H.; Hou, R.; Lou, X.; Xia, F. Role of Outer Surface Probes for Regulating Ion Gating of Nanochannels. *Nat. Commun.* **2018**, *9*, No. 40.
(12) Liu, N.; Jiang, Y.; Zhou, Y.; Xia, F.; Guo, W.; Jiang, L. Two-Way Nanopore Sensing of Sequence-Specific Oligonucleotides and Small-Molecule Targets in Complex Matrices Using Integrated DNA Supersandwich Structures. *Angew. Chem. Int. Ed.* **2013**, *52*, 2007−2011.
(13) Yu, P.; He, X.; Zhang, L.; Mao, L. Dual Recognition Unit Strategy Improves the Specificity of the Adenosine Triphosphate (ATP) Aptamer Biosensor for Cerebral ATP Assay. *Anal. Chem.* **2015**, *87*, 1373−1380.
(14) Zhang, K.; Xiong, T.; Wu, F.; Yue, Q.; Ji, W.; Yu, P.; Mao, L. Real-time and In-situ Intracellular ATP Assay with Polyimidazolium Brush-modified Nanopipette. *Sci. China Chem.* **2020**, *63*, 1004−1011.
(15) Melani, A.; Turchi, D.; Vannucchi, M. G.; Cipriani, S.; Gianfriddo, M.; Pedata, F. ATP Extracellular Concentrations are Increased in the Rat Striatum During in Vivo Ischemia. *Neurochem. Int.* **2005**, *47*, 442−448.
(16) Youn, Y.; Lee, C.; Kim, J.; Chang, Y.; Kim, D.; Yoo, K. Selective Detection of Single-Stranded DNA Molecules Using a Glass Nanocapillary Functionalized with DNA. *Anal. Chem.* **2016**, *88*, 688−694.
(17) Wang, X.; Zhao, H.; Chen, Z.; Luo, F.; Guo, L.; Qiu, B.; Lin, Z.; Wang, J. A Homogeneous Photoelectrochemical Hydrogen Sulfide Sensor Based on the Electronic Transfer Mediated by Tetrasulfophthalocyanine. *Analyst* **2020**, *145*, 3543−3548.
(18) Zhan, W.; Julio, A.; Richard, M. Electrochemical Sensing in Microfluidic Systems Using Electrogenerated Chemiluminescence as a Photonic Reporter of Redox Reactions. *J. Am. Chem. Soc.* **2002**, *124*, 13265−13270.
(19) Wang, H.; Ruan, Y.; Zhu, L.; Shi, X.; Zhao, W.; Chen, H.; Xu, J. An Integrated Electrochemical Nanodevice for Intracellular RNA Collection and Detection in Single Living Cell. *Angew. Chem. Int. Ed.* **2021**, *133*, 13352−13358.
(20) Zhang, K.; He, X.; Liu, Y.; Yu, P.; Fei, J.; L, M. Highly Selective Cerebral ATP Assay Based on Micrometer Scale Ion Current Rectification at Polyimidazolium-Modified Micropipettes. *Anal. Chem.* **2017**, *89*, 6794−6799.

https://doi.org/10.1021/acsami.2c10776
ACS Appl. Mater. Interfaces 2022, 14, 37222−37228